Oncogene (2003) 22, 5238–5251

www.nature.com/onc

Loss of p53 function accelerates acquisition of telomerase activity in indefinite lifespan human mammary epithelial cell lines

Martha R Stampfer*,[1], James Garbe[1], Tarlochan Nijjar[1], Don Wigington[1], Karen Swisshelm[2] and Paul Yaswen[1]

[1]*Lawrence Berkeley National Laboratory, Life Sciences Division, Bldg. 70A1118, Berkeley, CA 94720, USA;* [2]*Department of Pathology, University of Washington, Seattle, WA 98195, USA*

We describe novel effects of p53 loss on immortal transformation, based upon comparison of immortally transformed human mammary epithelial cell (HMEC) lines lacking functional p53 with closely related p53(+) lines. Our previous studies of p53(+) immortal HMEC lines indicated that overcoming the stringent replicative senescence step associated with critically short telomeres (agonescence), produced indefinite lifespan lines that maintained growth without immediately expressing telomerase activity. These telomerase(−) 'conditionally immortal' HMEC underwent an additional step, termed conversion, to become fully immortal telomerase(+) lines with uniform good growth. The very gradual conversion process was associated with slow heterogeneous growth and high expression of the cyclin-dependent kinase inhibitor $p57^{Kip2}$. We now show that p53 suppresses telomerase activity and is necessary for the p57 expression in early passage p53(+) conditionally immortal HMEC lines, and that p53(−/−) lines exhibit telomerase reactivation and attain full immortality much more rapidly. A p53-inhibiting genetic suppressor element introduced into early passages of a conditionally immortal telomerase(−) p53(+) HMEC line led to rapid induction of hTERT mRNA, expression of telomerase activity, loss of p57 expression, and quick attainment of uniform good growth. These studies indicate that derangements in p53 function may impact malignant progression through direct effects on the conversion process, a potentially rate-limiting step in HMEC acquisition of uniform unlimited growth potential. These studies also provide evidence that the function of p53 in suppression of telomerase activity is separable from its cell cycle checkpoint function.
Oncogene (2003) **22,** 5238–5251. doi:10.1038/sj.onc.1206667

Keywords: immortal transformation; telomerase; telomeres; TGFβ; genomic instability; conversion; p53

*Correspondence: MR Stampfer; E-mail: mrstampfer@lbl.gov
Accepted 4 April 2003

Introduction

Cells obtained from normal human somatic tissues display a finite lifespan *in vitro*; immortal transformation virtually never occurs spontaneously and has been extremely difficult to achieve even after exposure to physical carcinogens. In contrast, immortal lines can be obtained from culture of tumor-derived cells. Immortality has been suggested to be critical for malignancy since development of invasive carcinomas involves accumulation of multiple derangements in cellular growth control over an extended time-frame, and replicative senescence normally halts growth before such error accumulation is possible (Bacchetti, 1996). Understanding the molecular derangements that produce cells with an unlimited lifespan *in vivo* may consequently elucidate key steps involved in malignant transformation.

Immortal and malignant transformation of human cells has been shown to involve disruption of pathways associated with p53 and retinoblastoma (RB), as well as altered regulation of telomerase expression. Mutations in the p53 gene are found in around 50% of all human cancers, and in 15–30% of human breast cancers (Sjogren *et al*., 1996; Iacopetta *et al*., 1998). Mutations in the RB gene are uncommon in breast cancers, but alterations in expression or function of molecules controlling RB activity; e.g., the cyclin-dependent kinase inhibitors (CKIs) $p16^{INK4a}$ and $p27^{Kip2}$, and the cyclins D1 and E, are common (Buckley *et al*., 1993; Keyomarsi and Pardee, 1993; Bartkova *et al*., 1994; Weinstat-Saslow *et al*., 1995). p16 expression is absent in around 30–40% of tumors, frequently as a consequence of gene silencing (Herman *et al*., 1995; Brenner *et al*., 1996). Changes in p27 expression are associated with more advanced breast tumors (Catzavelos *et al*., 1997; Porter *et al*., 1997). Unlike normal human tissues, the vast majority of human tumors, including breast cancers, express telomerase activity. Telomerase activity is first detected in some breast carcinomas *in situ*, suggesting that its activation is an early event in cancer progression (Sugino *et al*., 1996; Bednarek *et al*., 1997; Poremba *et al*., 1999; Shpitz *et al*., 1999).

We have developed a human mammary epithelial cell (HMEC) system to study how normal growth control

processes are deranged in the course of immortal and malignant transformation (Hammond *et al*., 1984; Stampfer and Bartley, 1985; Stampfer and Yaswen, 2000; Stampfer and Yaswen, 2001). Reduction mammoplasty-derived HMEC grown in the serum-free medium MCDB 170, or the serum-containing medium, MM, show active growth for 15–30 population doublings (PDs), followed by a proliferative arrest associated with expression of high p16 levels, senescence associated β-galactosidase (SA-βgal) activity, and a mean terminal restriction fragment (TRF) length of $\sim$8–6 kb (Brenner *et al*., 1998; Garbe *et al*., 1999). In MCDB 170, a small number of cells undergo a spontaneous self-selection process. Postselection HMEC maintain good growth for an additional 30–70 PD and do not express p16, a phenotype correlated with hypermethylation of the p16 promoter (Hammond *et al*., 1984; Stampfer, 1985; Brenner *et al*., 1998). Postselection HMEC cease growth with a mean TRF of $\sim$5 kb, and expression of SA-βgal (Stampfer *et al*., 1997; Brenner *et al*., 1998; Romanov *et al*., 2001). This second, extremely stringent proliferation barrier, termed agonescence, is associated with widespread karyotypic aberrations, particularly telomere associations, consistent with telomere dysfunction due to critically short telomeres (Romanov *et al*., 2001; Tlsty *et al*., 2001). Agonescence is how the telomere-length-based proliferative barrier presents when p53 is functional, whereas crisis is how this barrier presents when p53 is not functional (manuscript in preparation).

Very rare immortal transformation of MM-grown HMEC from specimen 184 was achieved following exposure to the chemical carcinogen benzo(a)pyrene (Stampfer and Bartley, 1985). Carcinogen-treated HMEC produced several different extended life (EL) cultures that ceased growth with mean TRF $\sim$5 kb, except for two cells that overcame agonescence and gave rise to two lines of indefinite lifespan, 184A1 and 184B5 (Stampfer and Bartley, 1985, 1988). Karyotypic analysis indicated distinct clonal origins, and a very low level of genomic instability, in both cell lines (Walen and Stampfer, 1989). Like most breast tumor cells, neither immortal line has a known defect in the expression or phosphorylation of RB, or in the sequence of p53 (Lehman *et al*., 1993; Sandhu *et al*., 1997). Similar to their finite lifespan EL precursors, both lines lack expression of p16 and contain a stable form of the p53 protein. Neither line displays sustained anchorage-independent growth, growth factor independence, or tumorigenicity.

Examination of the p53(+) immortal 184A1 and 184B5 lines uncovered the previously undescribed process of conversion (Stampfer *et al*., 1997). The newly emerged immortal lines showed no telomerase activity and continued telomere erosion with passage. Like finite lifespan HMEC, they exhibited no sustained growth in TGFβ, but unlike the finite lifespan HMEC, they expressed high levels of the CKI p57 during G0 arrest (Nijjar *et al*., 1999). When the mean TRF of 184A1 declined to $\sim$3 kb, a severe growth constraint became prominent, tightly associated with a failure to down-regulate p57 after release from G0. When the mean TRF declined to $\sim$2 kb, poor but sustained growth in TGFβ could be seen in some cells, and weak telomerase activity could be detected in some clonal isolates. Subsequently, the cell population (both mass cultures and repeatedly cloned isolates) gradually converted to a phenotype with: (1) increasing levels of telomerase activity; (2) more uniform and rapid growth; (3) decreasing levels of p57 in G0-arrested and cycling cells, and (4) increasing numbers of cells with progressively better growth in TGFβ. These studies have indicated that overcoming agonescence and attaining full immortality in HMEC does not *require* mutations in either p53 or RB, nor *immediate* expression of telomerase activity; telomerase reactivation can occur subsequent to attaining immortal potential.

In this report, we examined the effect of p53 on the conversion of immortally transformed HMEC. Comparison of three p53(+) HMEC lines, 184A1, 185B5, and the newly generated 184AA4 line, with two newly generated p53(−/−) lines, 184AA2 and 184AA3, suggested that lack of p53 resulted in expression of telomerase activity soon after attaining immortality, absence of p57 expression, and accelerated attainment of full immortality. The direct role of p53 in suppressing telomerase activity in newly emerged immortal lines, and permitting p57 expression, was then demonstrated through the introduction of a p53-inhibiting genetic suppressor element (GSE) into early passage, telomerase(−), conditional immortal 184A1. These studies characterize a new role of p53 in suppression of telomerase activity and malignant progression. They also indicate why the conversion process was not previously uncovered, as almost all other human lines immortally transformed *in vitro* lack p53 function.

Results

p53 gene status and function differ in four distinct immortally transformed HMEC lines obtained from the same EL culture

To study the role of p53 in HMEC immortal transformation, the physical and functional status of p53 was examined in the four immortal HMEC lines, all derived from EL 184Aa, shown in Figure 1a and described in Material and methods. Previous studies have indicated that the wild-type p53 present in postselection 184, EL 184Aa, and 184A1 has a stable conformation readily detectable on immunoblots, whereas the short-lived p53 protein from 184 fibroblasts (184Fb) is less abundant, but still detectable on the same blots. Immunoblot analysis of the 184AA2 and 184AA3 cell lines showed no p53 expression even after long exposure, whereas 184AA4, similar to 184 and 184A1, showed a high level of p53 expression characteristic of stable p53 (Figure 1b). Further analysis by sequencing and Southern hybridization indicated that both 184AA2 and 184AA3 have viral insertions within the first intron of one allele of the p53 gene and that no normal p53 alleles are present in either

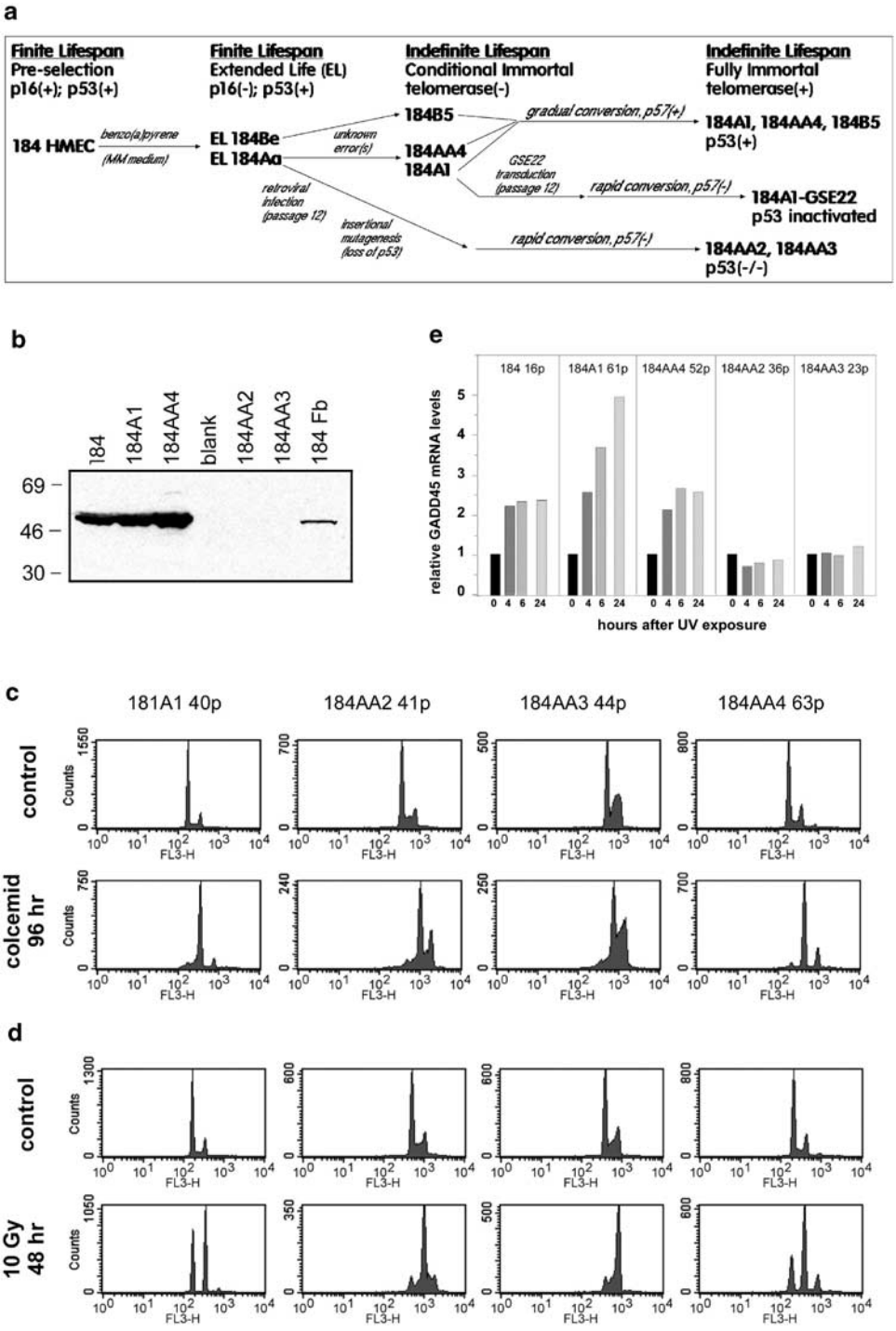

Figure 1 Derivation and p53 expression and function of immortalized HMEC lines. (**a**) Schematic diagram of derivation of immortal HMEC lines. See Material and methods for details. (**b**) Cell lines 184AA2 and 184AA3 do not express p53 protein. Protein lysates were prepared from postselection 184 at passage 13, 184A1 at passage 14, 184AA4 at passage 24, 184AA2 at passage 26, 184AA3 at passage 23, and 184 fibroblasts at passage 7. Positions of the molecular weight markers are indicated. (C,D,E) Cell lines 184AA2 and 184AA3 exhibit altered p53-dependent responses. FACS analysis was performed following exposure to (**c**) 50 ng/ml colcemid and (**d**) 10 Gy of ionizing radiation. (**e**) Northern analysis of UV-induced GADD45 mRNA expression in samples harvested at the indicated times following UV exposure. Densometric scans of hybridized signals were normalized to those of rRNA

184AA2 or 184AA3 (data not shown). These data indicate that both these HMEC lines are p53(−/−).

The functional status of p53 was determined by assaying the ability of the individual cell lines to: (1) arrest growth after exposure to the microtubule destabilizing agent colcemid; (2) arrest growth after exposure to X-irradiation; (3) accumulate GADD45 mRNA following UV exposure. Following 96 h of

Table 1 Cell cycle distribution and DNA synthesis in p53(+) and p53(−/−) HMEC lines following exposure to colcemid or X-rays

	Control		*Colcemid 96 h*		*Control*		*X-ray 48 h*	
Cell line	*% total*	*% BrdU+*	*% total*	*% BrdU++*	*% total*	*% BrdU+*	*% total*	*% BrdU+*
184A1								
<2n	0.2	0.0	9.1	0.4	0.3	0.0	0.2	0.0
2n	66.9	7.2	5.5	0.2	64.8	6.8	41.0	0.3
2n>4n	17.5	16.8	21.6	0.5	18.0	17.3	1.0	0.3
4n	13.6	8.8	50.7	1.3	14.1	9.1	52.1	1.4
>4n	1.7	1.0	13.1	2.9	2.8	1.7	5.6	1.9
Total	100.0	33.8	100.0	5.2	100.0	35.1	100.0	3.9
184AA2								
<2n	1.7	0.3	2.2	0.4	1.6	0.4	0.5	0.2
2n	57.7	4.1	2.2	0.3	56.2	4.7	9.8	1.3
2n>4n	22.6	20.2	10.6	0.8	22.7	20.0	15.5	8.6
4n	13.6	6.4	4.6	0.4	14.7	8.1	45.0	7.6
>4n	4.4	2.6	80.4	21.4	4.8	3.1	29.1	18.8
Total	100.0	33.7	100.0	23.2	100.0	36.3	100.0	36.4
184AA3								
<2n	0.8	0.2	2.2	0.2	0.6	0.1	0.6	0.0
2n	45.0	3.4	4.4	0.2	50.1	3.9	9.5	0.2
2n>4n	36.7	35.6	7.3	0.5	27.4	26.3	29.0	9.0
4n	16.1	10.1	34.6	3.0	20.3	11.9	54.8	9.0
>4n	1.4	1.0	51.5	13.6	1.6	0.9	6.1	2.9
Total	100.0	50.3	100.0	17.4	100.0	43.1	100.0	21.1
184AA4								
<2n	0.3	0.1	0.3	0.2	6.6	0.1	0.7	0.0
2n	59.3	5.5	4.3	0.3	55.3	6.6	25.5	0.7
2n>4n	13.5	12.0	3.8	0.2	14.1	13.1	3.0	1.6
4n	18.3	10.9	69.5	1.1	18.3	10.8	53.8	2.8
>4n	8.5	4.5	22.1	3.8	5.7	3.1	17.0	4.3
Total	100.0	33.0	100.0	5.6	100.0	33.7	100.0	9.3

Randomly cycling populations were exposed to either colcemid (50 ng/ml) or X-rays (10 Gy) for the indicated times. Cells were labeled with 10 μM BrdU during the last 4 h of incubation, then harvested and prepared for FACS analysis. DNA content was determined by propidium iodide staining. BrdU(+) cells were identified using a fluorochrome-labeled anti-BrdU antibody

colcemid exposure, p53(+) 184A1 and 184AA4 contained DNA contents corresponding mostly to 4n, whereas p53(−/−) 184AA2 and 184AA3 contained >4n; 184AA2 and 184AA3 also showed greater ongoing DNA synthesis as evidenced by the continued incorporation of BrdU (Figure 1c, Table 1). At 48 h following X-irradiation, p53(+) 184A1 and 184AA4 arrested with DNA contents largely corresponding to 2n or 4n, with few cells in S phase (Figure 1d, Table 1). The presence of some tetraploid cells in 184AA4 cultures (see below) may account for some of the 8n population seen in these assays. In contrast, p53(−/−) 184AA2 and 184AA3 cells had peaks corresponding to 4n, but also showed broad distributions of DNA contents ranging from 2n to >4n; 184AA2 and 184AA3 also maintained DNA synthesis following X-irradiation. Finally, 184AA2 and 184AA3 showed no GADD45 induction, whereas the p53(+) HMEC exhibited 2–5-fold GADD45 induction 4–24 h following UV exposure (Figure 1e).

These analyses indicate that the 184AA2 and 184AA3 lines lack p53 expression and functional activities. Further, these data demonstrate that the abundant p53 protein present in the p53(+) HMEC lines is functional, but does not show checkpoint-arresting activities in the absence of activating stimuli such as irradiation or colcemid.

p53(−/−) HMEC lines 184AA2 and 184AA3 rapidly reactivate telomerase activity and attain full immortality

Prior analysis of the p53(+) 184A1 and 184B5 lines indicated that they underwent a gradual conversion process (Stampfer *et al*., 1997). The newly derived p53(−/−) 184AA2 and 184AA3 lines and p53(+) 184AA4 were now analysed at different passage levels for conversion associated phenotypes, that is, telomerase activity, mean TRF, growth in TGFβ, and p57 expression.

The conversion process in 184AA4 resembled that seen in 184A1. Both lines were derived from EL 184Aa, and were first detected in 184Aa populations at passages 13 and 9, respectively. No telomerase activity was detected in early passage 184AA4, while later passages showed a gradual increase in activity (Figure 2b and d). Mean TRF analysis of the earliest passage 184AA4 that could be examined, passage 23, showed a faint signal of <2.0 kb (Figure 2a and e), indicating a decline from the ~4–5 kb length in the parental 184Aa population at passage 13 (Stampfer *et al*., 1997), and consistent with

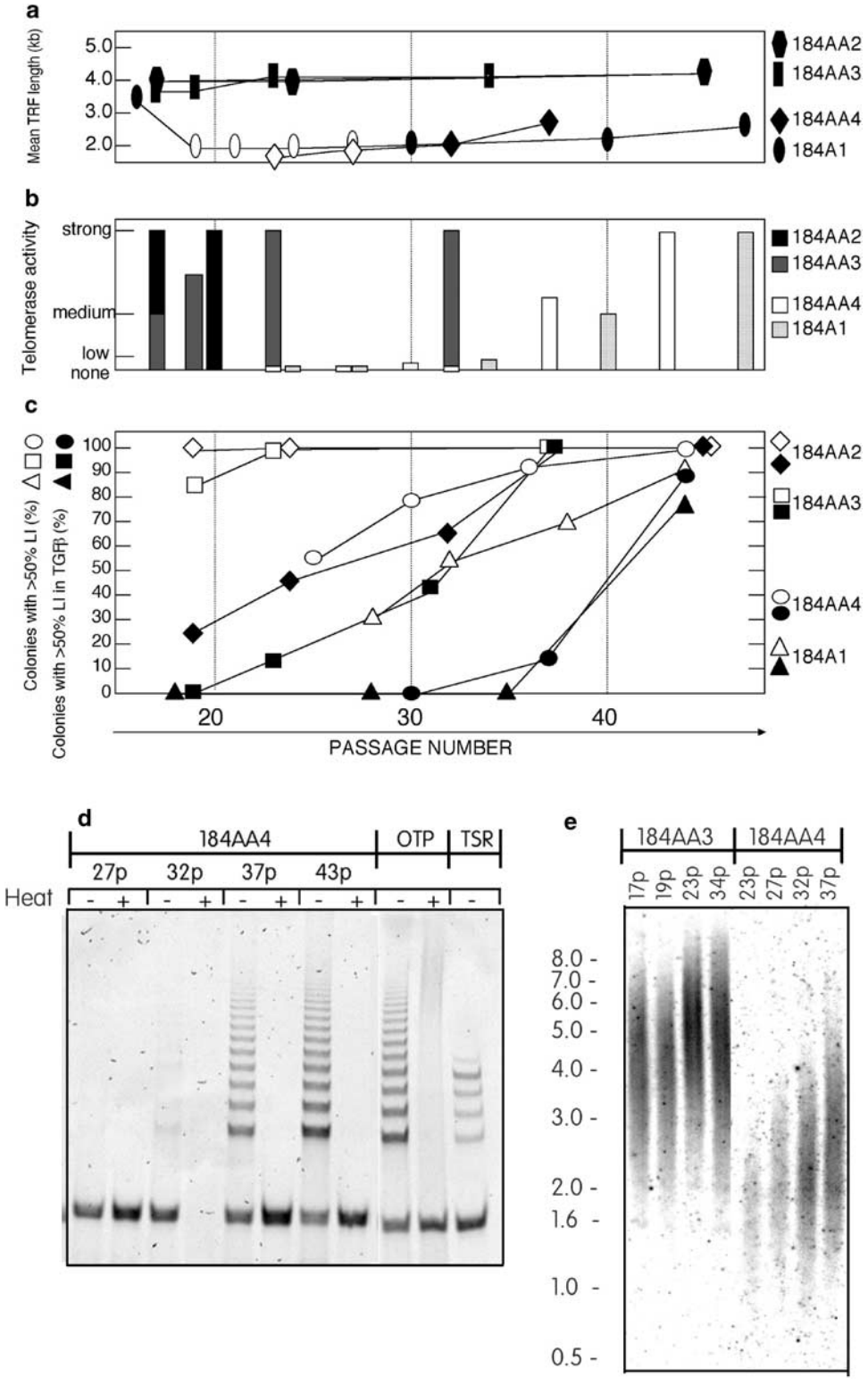

Figure 2 Conversion to full immortality is accelerated in p53(−/−) lines. Different passage levels of p53(+) 184A1 and 184AA4 and p53(−/−) 184AA2 and 184AA3 were assayed for (**a**) mean TRF length; (**b**) telomerase activity; (**c**) growth ±TGFβ. For mean TRF length, open symbols indicate that the signals were faint. For telomerase activity, semiquantitative values were obtained by comparing the levels of HMEC telomerase products generated to those generated for a constant number of 293 cells (1,000 cell equivalents). The following categories were used: None = no detectable telomerase products by phosphorimager analysis; low = approximately 10% of 293 control; medium = 25–50% of 293 control; strong = >75% of 293 control. LIs in colonies grown ±TGFβ were determined as described in experimental procedures. (**d**) Representative TRAP assay for 184AA4. (**e**) Representative TRF assays for 184AA3 and 184AA4

Table 2 Growth of 184AA2, 184AA3, 184AA4, and 184A1-GSE22 colonies at different passage levels in the absence or presence of TGFβ

	Labeling index (%)							
	TGFβ (−)				*TGFβ (+)*			
Cell line/passage	*<10*	*10–25*	*26–50*	*>50*	*<10*	*10–25*	*26–50*	*>50*
184AA2								
19	0	0	1	99	12	29	35	24
24	0	0	0	100	0	13	41	46
32	ND				7	12	28	64
45	0	0	0	100	0	0	0	100
184AA3								
17	TFTC				TFTC			
19	0	0	15	85	24	38	38	0
23	0	0	2	98	15	42	30	13
31	ND				14	21	34	43
37	0	0	0	100	0	0	0	100
184AA4								
23	TFTC				TFTC			
25	14	9	21	56	36	60	4	0
30	12	1	8	79	ND			
36/37	0	3	5	92	23	32	31	14
44	0	0	0	100	8	4	0	88
184A1-Babe								
14	15	37	30	18	94	6	0	0
17	16	20	30	34	91	6	2	0
20	32	8	32	29	65	23	11	0
184A1-GSE22								
14	17	26	25	32	24	27	25	24
17	13	11	22	54	40	18	23	19
21	4	12	10	74	39	21	18	22
25	0	0	0	100	36	16	17	32
30	0	0	0	100	12	5	21	62

A total of 200–10 000 single cells were seeded per 100 mm dish, and the labeling index $\pm$TGFβ in the ensuing colonies that contained >50 cells was determined as described in Materials and methods. At least 45 colonies were counted to determine percentage labeling index. ND = not determined; TFTC = too few colonies to count

the absence of telomerase activity. By passage 32, the ~2.0 kb TRF signal in 184AA4 became stronger, and then increased to ~3 kb by passage 37. 184AA4 growth capacity $\pm$TGFβ also gradually increased (Figure 2c and Table 2). Abundant p57 mRNA expression was seen during G0 arrest at passage 25 (Figure 3). Lower, but still detectable levels of p57 expression were present in passage 61 G0-arrested cells. In cycling 184AA4 populations, p57 expression was detectable at passage 25, but was greatly reduced compared to the G0-arrested cells; p57 was barely detectable in cycling 184AA4 at passage 61. Fully immortal passage 71 184AA4 did not display any anchorage-independent growth (Table 3). Altogether, these data indicate that p53(+) 184AA4 undergoes a gradual conversion process very similar to the p53(+) lines 184A1 and 184B5.

Unlike the p53(+) lines, p53(−/−)184AA2 and 184AA3 rapidly attained full immortality. 184AA2 displayed good initial growth and maintained good growth thereafter; 184AA3 displayed very slow initial growth, but achieved good uniform growth by passages 20–24 (Table 2). These initial observations indicated that these p53(−/−) lines did not undergo a very gradual

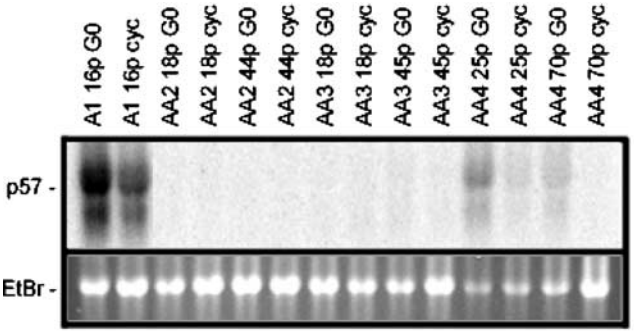

Figure 3 Cell lines 184AA2 and 184AA3 do not express p57 mRNA. p53(+) 184A1 and 184AA4 and p53(−/−) 184AA2 and 184AA3 were examined at the indicated early and late passages for p57 mRNA expression. Cells were arrested in G0 by removal of EGF from the medium and addition of the anti-EGF receptor antibody MAb225 for 48 h. Cycling cells were fed 48 and 24 h prior to harvest. The bottom panel indicates relative amounts of total RNA loaded in each lane, as judged by ethidium bromide staining

conversion process. To determine to what extent they did display conversion-associated properties, 184AA2 and 184AA3 were examined at different passage levels for telomerase activity, mean TRF length, growth

Table 3 Anchorage-independent growth of 184AA lines

Cell line	Passage#	Colony size distribution (% colonies/total cells seeded) 75–150 μm	> 150 μm
184AA2	19	0.58	0.04
184AA2	50	0.03	0.08
184AA3	19	0	0
184AA3	50	0.55	0.03
184AA4	71	0	0

Single cells (10^5) were suspended per 60 mm dish in methylcellulose as described in Materials and methods. The percent of cells capable of forming colonies at the indicated size was determined after 3 weeks

capacity ±TGFβ (Figure 2; Table 2), and p57 expression (Figure 3).

184AA2 already contained strong telomerase activity when assayed at passage 17. Consistent with telomerase activity being present, the mean TRF length remained at a stable value of ~4 kb from passage 17 through passage 45. 184AA2 did show the conversion-associated gradual acquisition of the ability to maintain growth in TGFβ. Although some cells were capable of maintaining growth in TGFβ at the earliest passages tested, uniform good growth was not present until after passage 32. In 184AA3, weak to medium telomerase activity was present at the earliest passage testable, passage 17, and strong activity was present by passage 23. The mean TRF increased from ~3.5 kb at passage 17 to a stabilized value of ~4 kb by passage 23. Some poor growth in TGFβ was present in passage 19 cells, but good uniform growth in TGFβ did not occur until after passage 31. Unlike the three p53(+) lines, no p57 mRNA expression was detected in either 184AA2 or 18AA3 at early or late passages, in G0 or in cycling populations (Figure 3). The capacity for anchorage-independent growth was already present in 184AA2, but not 184AA3, at passage 19. However, both 184AA2 and 184AA3 displayed anchorage-independent growth when examined at passage 50 (Table 3). Continued passage of 184AA3 may have selected for rare, pre-existent anchorage-independent cells, or promoted the generation of cells harboring this aberration.

Altogether, these data indicate that the behavior of early passages of both p53(−/−) lines significantly differed from that displayed by early passages of the p53(+) lines. The p53(−/−) lines expressed telomerase activity more rapidly, mean TRF lengths did not decrease below 3.5 kb, they quickly acquired uniform good growth potential, and p57 expression was totally absent. The p53(−/−) lines resembled the p53(+) lines in showing a gradual acquisition of increasing number of cells with progressively better growth capacity in TGFβ.

Inactivation of p53 expression in early passage conditionally immortal 184A1 produces rapid telomerase reactivation and attainment of full immortality

The capacity of both p53(−/−) lines to express telomerase activity rapidly, and their absence of p57 expression, suggested that these properties were the result of the lack of p53 function. To test this possibility directly, p53 function was inactivated in early passage 184A1 by transduction of the p53-inactivating GSE, GSE22 (Ossovskaya *et al*., 1996). The inhibition of p53 function in the 184A1-GSE22 culture was demonstrated by its failure to arrest fully after exposure to colcemid or X-irradiation (Figure 4).

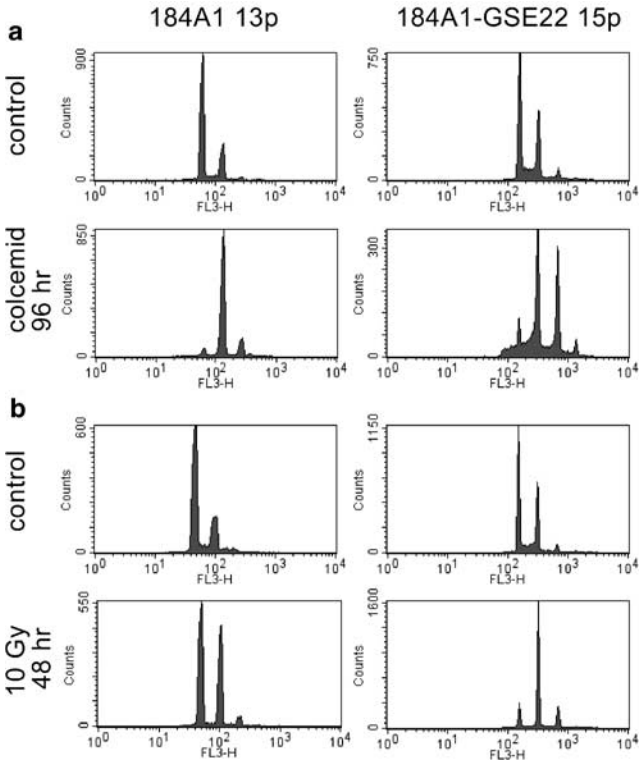

Figure 4 184A1 transduced with the dominant negative p53 GSE GSE22 at passage 12 (184A1-GSE22), shows reduced capacity for checkpoint arrest following exposure to (**a**) 50 ng/ml colcemid and (**b**) 10 Gy of ionizing radiation

184A1 transduced at passage 12 with GSE22 rapidly expressed telomerase activity and gained full immortality. As shown in Figure 5a, 184A1-GSE22 displayed intermediate levels of telomerase activity 7 days after the population was infected at passage 12, and strong activity was present by passage 19. As expected, the control, vector alone culture, 184A1-Babe, showed no telomerase activity at passage 12 or 16. Consistent with the TRAP assay results, quantitative RT–PCR assay showed a >10-fold increase in hTERT mRNA expression within two passages of GSE22 transduction (Figure 5b). Thus, inactivation of p53 function allowed rapid induction of hTERT and telomerase activity in conditionally immortal telomerase(−) HMEC. As shown in Figure 5c, the mean TRF length in 184A1-GSE22 showed a modest decline from ~5 kb at passage 13 to a stabilized length of ~4 kb by passage 25. The TRF signal never became faint nor declined below 4 kb. As shown in Table 2, 184A1-GSE22 did not undergo a prolonged slow growth phase; uniform good growth was present by passage 25. 184A1-GSE22 assayed up to passage 30 showed a gradual increase in the capacity to maintain growth in the presence of TGFβ. No p57 protein was expressed in the 184A1-GSE22 cycling

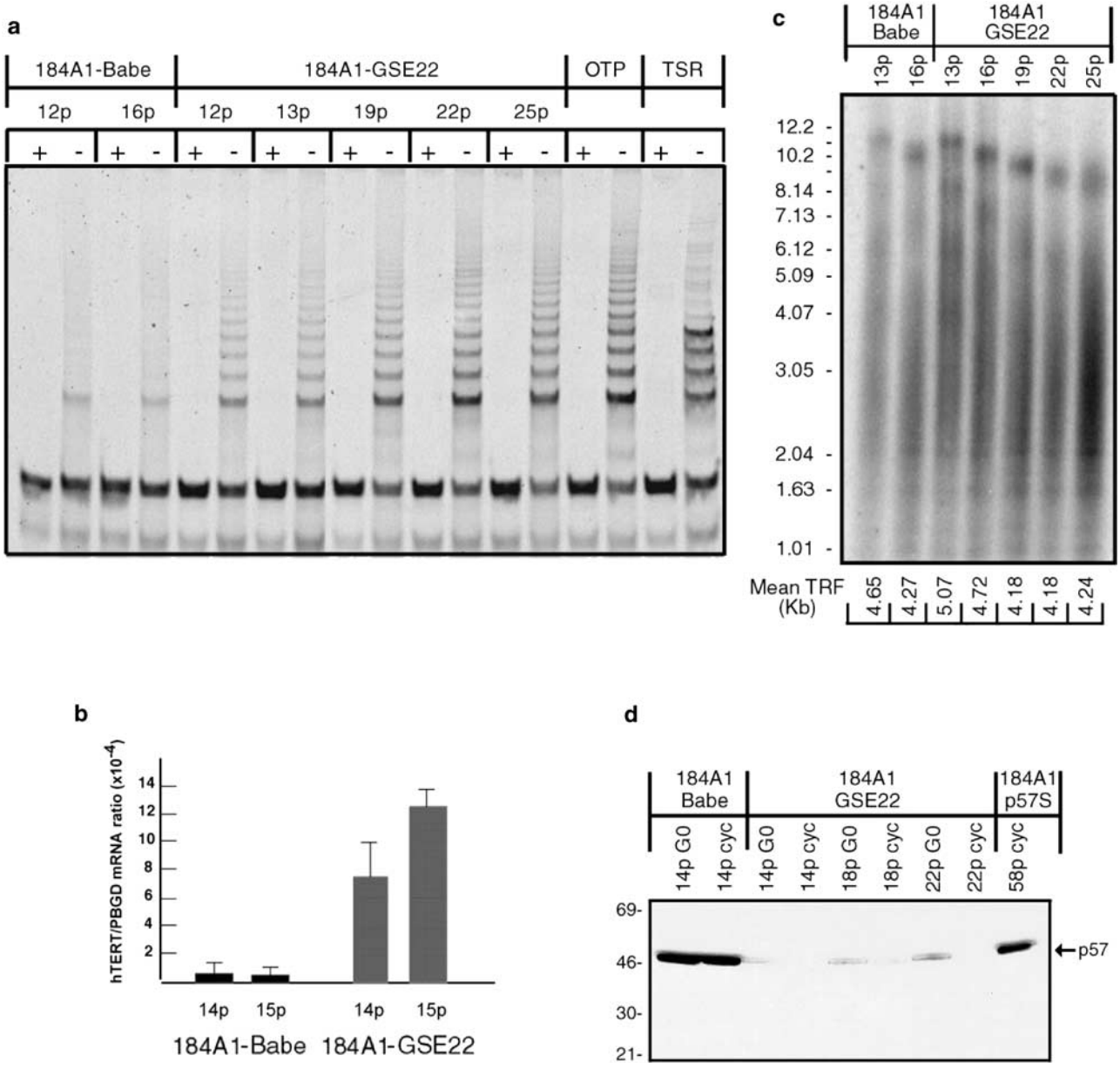

Figure 5 184A1 transduced with GSE22 shows rapid induction of telomerase activity, stabilization of telomere lengths, and reduction in p57 expression. Representative (**a**) TRAP (**b**) Quantitative RT–PCR for hTERT and (**c**) mean TRF results are shown for the184A1-Babe control and 184A1-GSE22 lines. Values at the bottom of (**b**) are mean TRF lengths calculated as described in Material and methods. (**d**) An immunoblot of total cell extracts probed with a specific anti-p57 antibody shows that p57 protein is downregulated in 184A1-GSE22 during G0 compared to the control cells, and that p57 protein is not expressed in cycling populations. An extract of 184A1 transduced with a p57 expression vector (p57S) is included to indicate the position of p57 protein on the gel

population at passages 14–22, in contrast to the abundant p57 at passage 14 in the 184A1-Babe control population (Figure 5d). Very low levels of p57 compared to 184A1-Babe could be seen in the G0-arrested cells. These results suggest that the high p57 expression in conditionally immortal HMEC is dependent upon expression of functional p53. The absence of p57 may in turn be responsible for the absence of a prolonged conversion-associated slow growth phase. Altogether, these data indicate that an absence of functional p53 can directly accelerate and/or circumvent the conversion process.

Karyotypic analysis shows different levels of initial chromosomal derangements and rates of genetic drift in the p53(−/−) and p53(+) cell lines

Loss of p53 function may contribute to malignant progression through an increase in genomic instability. Our previous studies indicated that the p53(+) 184A1 and 184B5 lines did not exhibit gross chromosomal instability as measured by karyotypic analysis or comparative genomic hybridization ((Walen and Stampfer, 1989); unpublished results). To determine if p53 loss was associated with greater genomic instability

Table 4 Karyotype analysis of 184AA lines

Cell line/ passage # analysed	*Chromosom mode*	*Range of chromosome #*	*Composite karyotype*	*Other aberrations/comments*	*Total # of cells analysed*
184AA2, p21	44	37–52	X,−4,−8,−9,?der(9), −11,−13, +der(15)x2,−16, −17,1−7, +der(20),−22, +4∼12mar	Small ring (4)[a], tas(4)[a], minutes(3)[a]	27
184AA2, p47	76	71–78	XX, +1, +1, +3, +7, +9, +der(9)x2, +der(11), der(15), +19,−17,−17+20, +der(2) x2, +21, +21,−22, +19∼22mars	Most cells with 1–3 min	26
184AA3, p23	63	58–71	X,der(X)add(Xp22.3),−1, +der(1)t(?;p21)x2,−4,−6,−9,−12,−13,−3, +der(13) add(q34),−15,−15, +der(15) ?i(q10), +3∼5mar	Small ring may be derived from chromosome 16 or 19	22
184AA3, p45	86	77–88	Similar to p23	No ring, minutes (10)[a], dicentrics occasionally observed. Some markers consist of 1q	20
184AA4, p26	45	42–49 70–81	X,−4,−6,−6,12, +der(15), +4∼10mar	 4/25 cells tetraploid with multiple double minutes/dicentrics	25
184AA4, p56	44	31–56 87	−X,−1−1,i(1)(p10) -−6,−8,−9,−10, −16,−18,−19+5∼7mar	No evidence of double minutes or dicentrics 1/21 cell tetraploid, similar, duplicated markers as in near diploids	24

[a]Number of cells in which the particular aberration was detected.

in our HMEC lines, the karyotypes of the newly generated 184AA2, 184AA3, and 184AA4 were analysed at early and late passage levels for the extent of initial chromosomal alterations, and ongoing chromosomal instability.

184AA4 could first be examined at passage 26, when the population was still exhibiting poor heterogeneous growth. The karyotype was mostly near-diploid, with approximately 10% of cells near-tetraploid. Unlike early passage 184A1 and 184B5, numerous chromosomal aberrations were present, including four to nine marker chromosomes, evidence of double minutes, and many dicentrics (Table 4). However, examination of the good growing passage 56 population showed a less aberrant karyotype, which was mostly near-diploid, with only three to four of the largest marker chromosomes present, and no evidence of dicentric or double minute chromosomes. A pronounced difference between the early and late passage 184AA4 cells was the absence of any detectable whole chromosome 1 in the late passage cells, coincident with the appearance of an iso-chromosome 1p. The absence of increasing genomic instability with passage suggests that the cells that maintained proliferative potential harbored fewer aberrations.

184AA2, first examined at passage 21, exhibited numerous chromosomal aberrations. The karyotype was near-diploid, with derivative chromosomes 15 and 20, 4–12 marker chromosomes, a small ring chromosome, the appearance of telomere association (tas), and minute, possibly acentric chromosomes (Table 4). Greater than 50% of the cells analysed contained likely identical large marker chromosomes. When examined again after approximately 80 additional PD (passage 47) the karyotype was now hyper-triploid, with an increased number of derivative and marker chromosomes. Most cells at both early and late passages exhibited one to three minute chromosomes. There was no identifiable chromosome 17, wherein the p53 gene is located at band p13.1.

184AA3, first examined at passage 23, also contained numerous chromosomal aberrations. The cells were hypo-triploid, with derivative chromosomes X, 13, and 15, as well as five to eight marker chromosomes. The three largest markers appeared to consist of material from the long arm of chromosome 1, indicating the presence of six or more copies of the entire or a large portion of 1q (Table 4). One or more large marker chromosomes, likely derived from the long arm of chromosome 1, were observed in greater than 70% of the early passage cells, suggesting a clonal origin of this line. After an additional approximately 70 PD (passage 45), the karyotype showed further chromosome complexity, with a modal chromosome number of 86 and an increased number of marker chromosomes and minute chromosomes. These results with the p53(−/−) lines indicate both a high level of initial chromosomal derangements, as well as increasing chromosomal instability with continued passage.

Discussion

Our previous work has described the process of conversion, a novel step associated with telomerase reactivation in HMEC that have *already overcome all senescence barriers and gained immortal potential* (Stampfer *et al*., 1997; Garbe *et al*., 1999; Nijjar *et al*., 1999; Nonet *et al*., 2001; Stampfer and Yaswen, 2001). These prior studies investigated HMEC that retained wild-type p53 and p53 functional activity following immortalization induced by a chemical carcinogen and/or a putative breast cancer oncogene, ZNF217. In this report, we examined the process of conversion in

immortalized HMEC lacking p53 expression and/or function. We show that newly immortalized HMEC lacking p53 exhibit rapid telomerase reactivation following immortalization, and that p53 suppresses telomerase activity and is required for p57 expression in early passage immortalized HMEC lines. These data expand the known roles of p53 in suppressing transformation. They may also explain why the conversion process was not previously uncovered, as almost all other human systems of *in vitro* immortalization use cells lacking p53 function (Band *et al*., 1991; Shay *et al*., 1993; Shay *et al*., 1995; Gao *et al*., 1996; Gollahon and Shay, 1996; Cao *et al*., 1997).

In our p53(+) HMEC, newly emerged indefinite lifespan lines initially exhibit little or no detectable telomerase activity. The conversion process involves a prolonged period of poor growth coincident with high expression of p57 and a mean TRF of <3 kb. In contrast, the p53(−/−) lines described here rapidly attained full immortality. Some telomerase activity was present at the earliest passage levels that could be assayed, mean TRF length did not decline below 3.5 kb, and uniform good growth was attained within 5–10 passages following isolation of these cell lines; furthermore, no p57 was expressed. The direct role of p53 in these differences was demonstrated by inhibiting p53 function in early passage conditionally immortal p53(+) 184A1 by transduction with the p53-inhibiting GSE22. 184A1-GSE22 rapidly expressed hTERT and telomerase activity and downregulated p57 expression. The fully immortal phenotype was present by passage 25, compared to passage 40 in control 184A1 cultures. Thus, the absence of p53 function greatly accelerated and/or circumvented the conversion process, and generated aggressively growing cells rapidly following the overcoming of all senescence barriers. A similar acceleration of telomerase reactivation was previously reported when p53 was inactivated in early passage 184A1 through transduction of the SV40-LgT antigen (Garbe *et al*., 1999).

The rapid expression of hTERT and telomerase activity in 184A1 transduced with GSE22 provides direct evidence that p53 plays a role in suppression of endogenous telomerase activity. However, preliminary experiments showing that introduction of GSE22 does not activate strong telomerase activity in postselection 184 or EL 184Aa (unpublished results) indicate that abrogation of p53 expression/function alone is not sufficient for expression of telomerase activity. Thus, overcoming agonescence may involve the occurrence of derangements that provide a *potential* to express telomerase activity, but where p53 remains present and functional, it may inhibit telomerase activity. This inhibition could occur through effects on hTERT transcriptional activation and/or direct association with other proteins in the telomerase complex (Li *et al*., 1999; Xu *et al*., 2000). In the p53(+) situation, telomerase reactivation was not observed prior to the lines attaining an extremely short telomere length, mean TRF <2.5 kb, and a very faint TRF signal. However, the p53(−/−) lines did not need to attain mean TRF lengths <3 kb prior to expressing telomerase activity, and indeed never acquired such short telomeres. p53(+) telomerase(−) conditionally immortal HMEC may require an as yet undefined alteration that occurs when the TRF reaches <3 kb, in order to overcome a p53-imposed inhibition of telomerase expression and/or activity. The ability of p53 to suppress telomerase activity may exemplify the potential of p53 to express functional activities in the absence of conditions that lead to its activation (Albrechtsen *et al*., 1999). In this regard, the higher p53 protein levels in post- vs preselection HMEC might compensate for the loss of p16 expression by increasing surveillance and suppression of genes favoring transformation, such as hTERT. Similar to what we have shown here for the p53(+) immortal HMEC lines, the stable p53 present in the postselection HMEC does not show checkpoint-arresting activities in the absence of activating stimuli (manuscript in preparation).

The earlier acquisition of TGFβ resistance in the p53(−/−) vs p53(+) lines is likely a consequence of their earlier expression of telomerase activity. We have shown that retroviral transduction of hTERT can confer gradual TGFβ resistance, over 10–20 passages, to telomerase(−) early passage conditionally immortal 184A1 (Stampfer *et al*., 2001). In both the p53(+) and p53(−/−) lines, most cells showed good uniform growth in TGFβ by around 15 passages following the first detection of telomerase activity. 184A1-GSE22 also showed a gradual increase in TGFβ resistance over the 13 passages in which it was assayed. Altogether, these data indicate that newly emerged immortal HMEC lines can gradually gain resistance to TGFβ growth arrest after acquiring telomerase activity, independent of p53 function.

A major distinction between our p53(+) and p53(−/−) HMEC lines is the absence of p57 expression when p53 function is lacking. p57 is readily detected in G0-arrested p53(+) conditionally immortal HMEC; the slow growth phase of conversion, which occurs when the mean TRF declines to <3 kb, is tightly correlated with a failure to downregulate p57 upon release from G0. We have hypothesized that this lack of p57 downregulation is signaled by the increasingly shortened telomere, since previous studies demonstrated that retroviral introduction of hTERT into passage 12 184A1 (mean TRF 4–5 kb) precludes further telomere erosion and prevents both expression of p57 in the cycling cell population and the slow growth phase of conversion (Nijjar *et al*., 1999; Stampfer *et al*., 2001). Similarly, we now show that inactivation of p53 function in passage 12 184A1 with GSE22: (1) prevented TRF decline below 4 kb; (2) prevented p57 expression in the cycling population; (3) produced nearly complete downregulation of the pre-existing levels of p57 expressed in G0-arrested cells; (4) eliminated the slow growth phase of conversion. The absence of p57 expression in the cycling populations of 184AA2, 184AA3, and 184A1-GSE22 could be attributed to the fact that their mean TRF length never declined below 3.5 kb. However, 184AA2 and 184AA3 also did not express any p57 in G0-arrested populations, and 184A1-GSE rapidly downregulated the pre-existing

G0-associated p57. If a conversion process occurs *in vivo*, whether or not p57 is expressed could significantly affect disease progression by influencing growth rate. Thus, the absence of p57 expression in the p53(−/−) cultures could have implications for the clinical course of p53(−/−) tumors.

Only 15–30% of primary human breast cancers contain mutations in the p53 gene, but these cancers have a significantly worse prognosis than those with wild-type p53 (Sjogren *et al*., 1996; Iacopetta *et al*., 1998; Roos *et al*., 1998). Where examined, p53 mutations generally occur early in breast cancer progression, being present in associated ductal carcinoma *in situ* lesions (Done *et al*., 1998). Our *in vitro* data showing that p53 loss is directly responsible for more rapid attainment of telomerase activity, and aggressive growth potential, is consistent with the *in vivo* data associating early p53 loss with poor prognosis, and suggests an additional mechanism whereby p53 loss can contribute to more aggressive cancer progression. Conversely, the presence of nonmutated p53 in the majority of human breast cancers could contribute to the generally less aggressive behavior of cancers such as breast and prostate that are largely p53 wild type.

The two p53(−/−) lines differed from the p53(+) lines in exhibiting ongoing genomic instability with continued passage in both chromosome number and presence of marker chromosomes. However, the p53(+) line 184AA4, unlike p53(+) 184A1 and 184B5, and similar to p53(−/−) 184AA2, 184AA3, and the p53(+) ZNF217-immortalized lines, evidenced numerous karyotypic aberrations when first examined. In contrast, 184A1 not only has few initial aberrations, it also shows few abnormalities even during conversion (Swisshelm, unpublished data), when it undergoes an extended period of proliferation with extremely short telomeres (mean TRF $\sim$2 kb). We hypothesize that the difference between these closely related p53(+) lines may be due to timing of the derangement(s) that permitted these cells to overcome agonescence. Agonescence entails widespread chromosomal aberrations, presumably resulting from telomeric associations among the critically short telomeres (Romanov *et al*., 2001). Agonescence-associated karyotypic abnormalities can be detected around two to four passages prior to the cessation of net proliferation in postselection HMEC. Cells that accumulate all the error(s) necessary for immortality *after* the onset of agonescence could harbor multiple karyotypic derangements due to passage through agonescence rather than immortal transformation or p53 loss. Ongoing chromosomal fusion-bridge-breakage cycles could then perpetuate the agonescence-induced genomic aberrations, even in the presence of functional p53 (Chang *et al*., 2001). The cultures that gave rise to our p53(+) lines that show numerous chromosomal rearrangements at early passages, 184AA4 and the ZNF217-immortalized lines, underwent agonescence prior to immortalization. Our p53(−/−) lines also arose in 184Aa cultures already undergoing agonescence. In contrast, cells that acquired all the errors necessary for immortalization *prior* to the onset of agonescence could avoid the agonescence-associated telomere dysfunction and retain a near-diploid karyotype. 184A1, which displays a near-diploid karyotype at early passages, appeared in EL 184Aa by passage 9, before agonescence would be encountered. 184B5, which has a few more initial aberrations than 184A1, appeared in EL 184Be around the time agonescence would be beginning. Possibly, even p53(−/−) immortal lines could harbor few initial chromosomal derangements if the p53 loss and immortalization events occur prior to attaining critically short telomeres. Similarly, subsequent p53 loss may not necessarily confer genomic instability if it occurs in lines immortalized without having undergone agonescence and fusion-bridge-breakage cycles. For example, we have reported that a 184A1 subclone malignantly transformed with SV40-T and H-*ras* did not exhibit genomic instability (Clark *et al*., 1988). Others have also reported that inactivation of p53 in finite lifespan and tumor-derived immortal human cells did not result in genomic instability (Bunz *et al*., 2002). We thus propose that the telomere dysfunction at agonescence may play a significant role in generating the karyotypic aberrations and genomic instability observed in both p53(+) and p53(−) human carcinomas. Consistent with this hypothesis is the observation that in breast cancer, as well as carcinomas of other organ systems, widespread karyotypic abnormalities are observed at early stages of carcinogenesis (Allred and Mohsin, 2000).

The maintenance of a near-diploid karyotype by 184A1, even during conversion, suggests the possibility that the errors that allowed 184A1 to avoid agonescence may also protect short telomere ends from telomeric associations, thus permitting the observed continued growth with extremely short telomeres. Protected short telomeres have been reported to be more genomically stable than unprotected telomeres of greater length (Chan and Blackburn, 2002; de Lange, 2002).

These studies demonstrating distinct molecular differences between p53(+) vs p53(−/−) immortally transformed HMEC, as well as our previous work, demonstrating obligate differences between finite lifespan and immortal HMEC, further emphasize that immortal, p53(−/−) cells significantly differ from normal finite lifespan cells, and should not be assumed to represent normal human cell biology. Indeed, each immortally transformed or tumor-derived cell line will likely contain unique combinations of several, potentially interactive, molecular derangements, which can produce significant deviation in cell cycle or signal transduction pathways, compared to the normal finite lifespan cell from which the line or tumor originated.

In summary, our generation of p53(+) and p53(−/−) immortally transformed HMEC lines from one individual has facilitated examination of the role of p53 in the conversion of postagonescent conditionally immortal HMEC to immortal fully telomerase expressing cell lines. The data thus far indicate that loss of p53 function may impact HMEC transformation *in vitro* by greatly abbreviating or circumventing the conversion process and yielding more aggressively growing cells in a shorter

time-frame. It will be of interest to determine if a similar mechanism also impacts the *in vivo* progression of human breast cancers differing in p53 status.

Material and methods

Cell culture

Finite lifespan 184 HMEC were obtained from reduction mammoplasty tissue that showed no epithelial cell pathology. Culture in serum-free MCDB 170 medium (MEGM, Clonetics Division of Cambrex, Walkersville, MD) or serum-containing MM medium was as described (Hammond *et al*., 1984; Stampfer, 1985). Extended lifespan 184Aa and 184Be, and immortal lines 184A1 and 184B5, emerged from 184 HMEC following benzo(a)pyrene exposure of primary cultures growing in MM as described (Stampfer and Bartley, 1985, 1988). 184Aa appeared as a single colony at passage 6, and showed complete loss of growth potential by passages 15–17 when grown in MCDB 170. 184A1 was detected in MM-grown 184Aa at passage 9 as good-growing morphologically distinct cells. 184B5 appeared in MM-grown 184Be at passage 6 as one small tightly packed patch of slowly growing cells.

Three newly generated HMEC lines were also used for these studies. A schematic outline of the generation of all these HMEC lines is presented in Figure 1a. 184AA4 appeared in MCDB 170-grown 184Aa at passage 13 as very slow-growing cell patches with a heterogeneous morphology. Later passage good-growing 184AA4 had a typical epithelial cobblestone morphology. 184AA2 and 184AA3 were detected in MCDB-170-grown 184Aa at passages 13 and 14, respectively, following exposure of 184Aa to high titer amphotrophic retrovirus at passage 12. 184AA2 first appeared as tight patches of refractile cells with many mitoses as well as larger flatter cells. It maintained good growth thereafter. 184AA3 first appeared as areas of small densely packed, grossly vacuolated and extremely slow-growing cells. Mass cultures began a gradual increase in growth rate by passages 16–18, with colonies becoming less densely packed with fewer grossly vacuolated cells. By passages 20–24, uniform good growth was attained, and cell morphology changed to more rounded and refractile.

Complete details on the derivation and culture of these HMEC can be found on our web site, www.lbl.gov/~mrgs.

Growth assays

HMEC were arrested in a G0 state by removal of EGF from the medium and exposure to 5 μg/ml of the anti-EGF receptor antibody MAb225 for 48 h as described (Stampfer *et al*., 1993). Random cycling cultures were fed 48 and 24 h prior to harvesting.

The ability to maintain growth in the absence or presence of TGFβ was assayed as follows: To detect colony forming efficiency (CFE), growth capacity, and heterogeneity of single cell-derived colonies, 200–10 000 cells were seeded per 100 mm dish, and cultures maintained for 14–20 days. [3 H]thymidine (0.5–1.0 μCi/ml) was then added for 24 h 4–7 h following refeeding, and labeled cells were visualized by autoradiography as described (Stampfer *et al*., 1993). CFE was determined by counting the number of colonies of >50 cells, and growth capacity by counting the percentage of labeled nuclei in these colonies. Uniform good growth was defined as a labeling index (LI) of $>50\%$. To determine growth capacity in TGFβ, 5 ng/ml TGFβ (R&D Systems, Minneapolis, MN, USA) in the presence of 0.1% bovine serum albumin (Sigma, St Louis, MO, USA), was added to some cultures for 10–14 days once the largest colonies contained 100–250 cells. Growth capacity per colony was determined as above. To detect very rare TGFβ-resistant cells in mass cultures, 10^5 cells were seeded per 100 mm dish, and TGFβ was added 24 h later for 10–14 days; control cultures received bovine serum albumin alone. Cells were then labeled and prepared for autoradiography as above. Cultures $\pm$TGFβ were also visually monitored at least twice weekly for growth, mitotic activity, and morphology.

Anchorage-independent growth was assayed by suspending 10^5 single cells in 5 ml of a 1.5% methylcellulose solution made up in MCDB 170, seeded onto 60 mm Petri dishes coated with Polyhema (Sigma). Plates were fed once a week, and colonies $>75\,\mu$m in diameter were counted and sized after 3 weeks using a calibrated ocular grid.

Retrovirus infection

The pBABE-GSE22-puro plasmid, encoding a p53 GSE corresponding to nucleotides 937–1199 in a retroviral vector (Ossovskaya *et al*., 1996) was provided by Dr Peter Chumakov, U IL, Chicago. Retroviral stocks were generated by transient co-transfection of the retroviral plasmid along with a plasmid encoding packaging functions into the 293 cell line (Finer *et al*., 1994). Retroviral supernatants were collected in serum-free MCDB 170 media containing 0.1% bovine serum albumin, filter sterilized and stored at -80°C. Viral infection of 184Aa and 184A1 cultures was in MCDB 170 media containing 0.1% bovine serum albumin and 2.0 μg/ml polybrene (Sigma).

Telomerase assays and TRF analysis

Cells for telomerase assays were fed 24 h prior to harvesting. Cell extracts were prepared by a modification of the detergent lysis method (Kim *et al*., 1994) and protein concentrations were determined using the Coomassie protein assay reagent (Pierce, Rockford, IL, USA). Telomerase activity was measured using the TRAP-EZE telomerase detection kit (Oncor, Inc.) using 2 μg of protein per assay. The ^{32}P-labeled telomerase products were detected using a phosphorimager (Molecular Dynamics, Sunnyvale, CA, USA) and semiquantitation was performed by comparing PCR signals from the HMEC extracts to signals from extracts of 293 cells.

DNA isolation and mean telomere restriction fragment (TRF) analysis were performed as previously described (Bodnar *et al*., 1996) with two modifications. Genomic DNA was isolated from cells and 3 μg was digested and resolved on 0.5% agarose gels. The separated DNA was transferred to a membrane and hybridized overnight to a ^{32}P-labeled telomere-specific probe $(CCCTAA)_4$, and washed to remove nonspecific hybrids. Signal was detected using a phosphorimager and quantitated using the Imagequant software program (Molecular Dynamics). Mean TRF length was calculated as described (Allsopp *et al*., 1992).

Immunoblot analysis

Protein lysates for analysis of p53 were collected from random cycling cells and processed for Western analysis as previously described (Nonet *et al*., 2001). Protein samples of 50 μg were resolved on a 4–12% polyacrylamide gradient gel and transferred to nitrocellulose membrane (Schleicher and Schuell, Keene, NH, USA). The membrane was blocked in TBST (25 mM Tris, pH 7.4, 137 mM NaCl, 2 mM KCl, 0.05% Tween-20) containing 5% nonfat powdered milk and incubated with a monoclonal antibody against p53 (Ab-6, Oncogene Research Products, Cambridge, MA, USA). Bind-

ing of primary antibodies was detected using HRP-conjugated anti-mouse IgG (Transduction Laboratories, Lexington, KY, USA) and visualized by chemiluminescence.

Quantitative RT–PCR

Quantitation of relative hTERT mRNA levels was performed using the LightCycler TeloTAGGGhTERT Quantitation Kit (Roche).

Northern blot analyses

To test for p53-dependent GADD45 expression, subconfluent cultures were exposed to UV irradiation (37 jules/cm2) followed by addition of fresh media. To test for p57 expression, cells were collected after 48 h of G0 arrest or in a randomly cycling state. Cultures were lysed directly into buffered guanidine thiocyanate solution. Total cellular RNA was purified and Northern blots prepared using 10 μg RNA per lane as previously described (Stampfer *et al*., 1993). The blots were hybridized to ^{32}P-labeled GADD45 or p57 cDNA probes (Kastan *et al*., 1992; Matsuoka *et al*., 1995). The hybridization signals were measured using a phosphorimager and quantitated using the Imagequant program (Molecular Dynamics), with the values normalized by comparison to ethidium bromide stained rRNA.

Checkpoint function analyses

To test for G2 checkpoint function, HMEC growing exponentially were incubated in media containing 50 ng/ml colcemid (Life Technologies, Bethesda, MD, USA). Treated cultures were refed every 24 h and samples collected at 0, 48, and 96 h. To test for G1 checkpoint function, HMEC were exposed to 10 Gy of ionizing radiation using a Pantak II X-ray generator. Irradiated and mock-irradiated cells were collected 24 and 48 h post-treatment. All cells were labeled with 10 μM BrdU for 4 h immediately prior to harvest. Analyses of BrdU incorporation and total DNA content was performed using a Becton-Dickinson flow sorter. All analysed events were gated to remove debris and aggregates. The fractions of BrdU(+) cells with specific DNA contents were determined by dividing the number of BrdU(+) events by the total number of gated events.

Karyotypic analysis

Log phase HMEC cultures were exposed overnight to a 0.01 μg/ml concentration of colcemid (Gibco). Following trypsinization, metaphase cells were collected in hypotonic buffer (3 : 1, 0.4% potassium chloride: 0.4% sodium citrate) and incubated at 37°C for 30 min followed by fixation in Carnoy's fixative (3 : 1, methanol : glacial acetic acid). Trypsin G-banding was performed following standard procedures.

Abbreviations

CFE, colony forming efficiency; CKI, cyclin-dependent kinase inhibitor; EL, extended life; GSE, genetic suppressor element; HMEC, human mammary epithelial cells; LI, labeling index; PDs, population doublings; RB, retinoblastoma; SA-βgal, senescence associated β-galactosidase; TRF, terminal restriction fragment.

Acknowledgements

We thank Michelle Wong and Gerri Levine for excellent technical help, and the Cell Genesys Corp. for providing the kat retroviral packaging system. Supported by NIH Grant CA-24844 (MRS, PY), the Office of Energy Research, Office of Health and Biological Research, US Department of Energy under Contract No. DE-AC03-76SF00098 (MRS, PY), the Susan G Komen Breast Cancer Foundation Grant 9742 (PY), California Breast Cancer Research Program Grant 4JB-0119 (MRS, PY), US Army DMAD-94-J-4028 (KS).

References

Albrechtsen N, Dornreiter I, Grosse F, Kim E, Weismuller L and Deppert W. (1999). *Oncogene,* **18,** 7706–7717.
Allred DC and Mohsin SK. (2000). *J. Mam. Gland Biol. Neoplasia,* **5,** 351–364.
Allsopp RC, Vaziri H, Patterson C, Goldstein S, Younglai EV, Futcher AB, Greider CW and Harley CB. (1992). *Proc. Natl. Acad. Sci. USA,* **89,** 10114–10118.
Bacchetti S. (1996). *Cancer Surveys,* **28,** 197–216.
Band V, DeCaprio J, Delmolino L, Kulesa V and Sager R. (1991). *J. Virol.,* **65,** 6671–6676.
Bartkova J, Lukas J, Muller H, Lutzhoft D, Strauss M and Bartek J. (1994). *Int. J. Cancer,* **57,** 353–361.
Bednarek A, Sahin A, Brenner AJ, Johnston DA and Aldaz CM. (1997). *Clin. Cancer Res.,* **3,** 11–16.
Bodnar AG, Kim NW, Effros RB and Chiu C-P. (1996). *Exp. Cell Res.,* **228,** 58–64.
Brenner AJ, Paladugu A, Wang H, Olopade OI, Dreyling MG and Aldaz CM. (1996). *Clin. Cancer Res.,* **2,** 1993–1998.
Brenner AJ, Stampfer MR and Aldaz CM. (1998). *Oncogene,* **17,** 199–205.
Buckley M, Sweeney K, Hamilton J, Sini R, Manning D, Nicholson R, deFazio A, Watts C, Musgrove E and Sutherland R. (1993). *Oncogene,* **8,** 2127–2133.
Bunz F, Fauth C, Speicher MR, Dutriaux A, Sedivy JM, Kinzler KW, Vogelstein B and Langauer C. (2002). *Cancer Res.,* **62,** 1129–1133.
Cao Y-A, Gao Q, Wazer DE and Band V. (1997). *Cancer Res.,* **57,** 5584–5589.
Catzavelos C, Bhattacharya N, Wilson JA, Roncari L, Shaw P, Yeger H, Morava-Protzner I, Kapusta L, Franssen E, Pritchard KI, Ung Y and Slingerland JM. (1997). *Nat. Genet.,* **3,** 227–230.
Chan SW-L and Blackburn EH. (2002). *Oncogene,* **21,** 553–563.
Chang S, Khoo C and DePinho RA. (2001). *Cancer Biol.,* **11,** 227–238.
Clark R, Stampfer M, Milley B, O'Rourke E, Walen K, Kriegler M and Kopplin J. (1988). *Cancer Res.,* **48,** 4689–4694.
de Lange T. (2002). *Oncogene,* **21,** 532–540.
Done SJ, Arneson NCR, zçelik H, Redston M and Andrulis IL. (1998). *Cancer Res.,* **58,** 785–789.
Finer MH, Dull TJ, Qin L, Farson D and Roberts MR. (1994). *Blood,* **83,** 43–50.
Gao Q, Hauser SH, Liu X-L, Wazer DE, Madoc-Jones H and Band V. (1996). *Cancer Res.,* **56,** 3129–3133.
Garbe J, Wong M, Wigington D, Yaswen P and Stampfer MR. (1999). *Oncogene,* **18,** 2169–2180.
Gollahon LS and Shay JW. (1996). *Oncogene,* **12,** 715–725.
Hammond SL, Ham RG and Stampfer MR. (1984). *Proc. Natl. Acad. Sci. USA,* **81,** 5435–5439.

Herman JG, Merlo A, Mao L, Lapidus RG, Issa J-PJ, Davidson NE, Sidransky D and Baylin SB. (1995). *Cancer Res.,* **55,** 4525–4530.

Iacopetta B, Grieu F, Powell B, Soong R, McCaul K and Seshadri R. (1998). *Clin. Cancer Res.,* **4,** 1597–1602.

Kastan MB, Zhan Q, El-Deiry WS, Carrier F, Jacks T, Walsh WV, Plunkett BS, Vogelstein B and Fornace Jr AJ. (1992). *Cell,* **71,** 587–597.

Keyomarsi K and Pardee AB. (1993). *Proc. Natl. Acad. Sci. USA,* **90,** 1112–1116.

Kim NW, Piatyszek MA, Prowse KR, Harley CB, West MD, Ho PLC, Coviello GM, Wright WE, Weinrich SL and Shay JW. (1994). *Science,* **266,** 2011–2015.

Lehman T, Modali R, Boukamp P, Stanek J, Bennett W, Welsh J, Metcalf R, Stampfer M, Fusenig N, Rogan E, Reddel R and Harris C. (1993). *Carcinogenesis,* **14,** 833–839.

Li H, Cao Y, Berndt MC, Funder JW and Liu J-P. (1999). *Oncogene,* **18,** 6785–6794.

Matsuoka S, Edwards MC, Bai C, Parker S, Zhang P, Baldini A, Harper JW and Elledge SJ. (1995). *Genes Dev.,* **9,** 650–662.

Nijjar T, Wigington D, Garbe JC, Waha A, Stampfer MR and Yaswen P. (1999). *Cancer Res.,* **59,** 5112–5118.

Nonet G, Stampfer MR, Chin K, Gray JW, Collins CC and Yaswen P. (2001). *Cancer Res.,* **61,** 1250–1254.

Ossovskaya VS, Mazo IA, Chernov MV, Chernova OB, Strezoska Z, Kondratov R, Stark GR, Chumakov PM and Gudkov AV. (1996). *Proc. Natl. Acad. Sci. USA,* **93,** 10309–10314.

Poremba C, Shroyer KR, Frost M, Diallo R, Fogt F, Schafer K-L, Burger H, Shroyer AL, Dockhorn-Dworniczak B and Boecker W. (1999). *J. Clin. Oncol.,* **17,** 2020–2026.

Porter PL, Malone KE, Heagerty PJ, Alexander GM, Gatti LA, Firpo EJ, Daling JR and Roberts JM. (1997). *Nat. Med.,* **3,** 222–225.

Romanov S, Kozakiewicz K, Holst C, Stampfer MR, Haupt LM and Tlsty T. (2001). *Nature,* **409,** 633–637.

Roos G, Nilsson P, Cajander S, Nielsen N-H, Arnerlöv C and Landberg G. (1998). *Int. J. Cancer,* **79,** 343–348.

Sandhu C, Garbe J, Bhattacharya N, Daksis JI, Pan C-H, Yaswen P, Koh J, Slingerland JM and Stampfer MR. (1997). *Mol. Cell. Biol.,* **17,** 2458–2467.

Shay JW, Tomlinson G, Piatyszek MA and Gollahon LS. (1995). *Mol. Cell. Biol.,* **15,** 425–432.

Shay JW, Wright WE, Brasiskyte D and Van Der Haegen BA. (1993). *Oncogene,* **8,** 1407–1413.

Shpitz B, Zimlichman S, Zemer R, Bomstein Y, Zehavi T, Liverant S, Bernehim J, Kaufman Z, Klein E, Shapira Y and Klein A. (1999). *Breast Cancer Res. Treat.,* **58,** 65–69.

Sjogren S, Inganas M, Norberg T, Lindgren A, Nordgren H, Holmberg L and Bergh J. (1996). *J. Natl. Cancer Inst.,* **88,** 173–182.

Stampfer MR. (1985). *J. Tissue Culture Methods,* **9,** 107–116.

Stampfer MR and Bartley JC. (1985). *Proc. Natl. Acad. Sci. USA,* **82,** 2394–2398.

Stampfer MR and Bartley JC. (1988). *Breast Cancer: Cellular and Molecular Biology* Dickson R and Lippman M. (eds) Kluwer Academic Publishers: Norwall, MA, pp. 1–24.

Stampfer MR, Bodnar A, Garbe J, Wong M, Pan A, Villeponteau B and Yaswen P. (1997). *Mol. Biol. Cell,* **8,** 2391–2405.

Stampfer M, Garbe J, Levine G, Lichsteiner S, Vasserot A and Yaswen P. (2001). *Proc. Natl. Acad. Sci. USA,* **98,** 4498–4503.

Stampfer MR, Pan CH, Hosoda J, Bartholomew J, Mendelsohn J and Yaswen P. (1993). *Exp. Cell Res.,* **208,** 175–188.

Stampfer MR and Yaswen P. (2000). *J. Mam. Gland Biol.Neoplasia,* **5,** 365–378.

Stampfer MR and Yaswen P. (2001). *Telomerase, Aging and Disease, Vol. 8: Advances in Cell Aging and Gerontology* Mattson M and Pandita T (eds) Elsevier: Amsterdam, pp. 103–130.

Sugino T, Yoshida K, Bolodeoku J, Tahara H, Buley I, Manek S, Wells C, Goodison S, Ide T, Suzuki T, Tahara E and Tarin D. (1996). *Int. J. Cancer,* **69,** 301–306.

Tlsty TD, Romanov SR, Kozakiewicz BK, Holst CR, Haupt LM and Crawford YG. (2001). *J. Mam. Gland Biol. Neoplasia,* **6,** 235–243.

Walen K and Stampfer MR. (1989). *Cancer Genet. Cytogenet.,* **37,** 249–261.

Weinstat-Saslow D, Merino M, Manrow R, Lawrence J, Bluth R, Wittenbel K, Simpson J, Page D and Steeg S. (1995). *Nat. Med.,* **1,** 1257–1260.

Xu D, Wang Q, Gruber A, Bjorkholm M, Chen Z, Zaid A, Selivanova G, Peterson C, Wiman KG and Pisa P. (2000). *Oncogene,* **19,** 5123–5133.